HADRON-HADRON INTERACTION FORM SU(2) LATTICE QCD

Toru T. Takahashi and Yoshiko Kanada-En'yo

Phys. Rev. D 82, 094506(2010)

2014年10月3日

MOTIVATION

- Two-color QCD で Nambu-Bethe-Salpeter amplitude を用いた potential の計算
- 4つの flavor, 異なる quark mass での potential から repulsive force の origin を探す
- Potential の operator dependence を見る

SETUP

- Quenched SU(2) QCD $24^3 \times 64$
- $\beta = 2.45$
- Wilson quark

  $\kappa = 0.1350, 0.1400, 0.1450, 0.1500, (0.1150, 0.1250)$

POTENTIALの導出①

CP-PACS collaboration(2005) の方法を用いる

S.Aoki et al. (CP-PACS Collaboration), Phys. Rev. D 71, 094504(2005)

- **Two-diquark collerator** W(**R**,t)

$$W_{ij,kl,\Gamma}(\mathbf{R}, t) \equiv$$

$$\sum_{\mathbf{x}} \langle D_{ij,\Gamma}(\mathbf{x}, t) D_{kl,\Gamma}(\mathbf{x}+\mathbf{R}, t) D^{\dagger}_{ij,\Gamma}(0,0) D^{\dagger}_{kl,\Gamma}(0,0) \rangle.$$

$$D_{ij,\Gamma}(\mathbf{x}, t) \equiv \varepsilon^{ab} q^a_i(\mathbf{x}, t) \Gamma q^b_j(\mathbf{x}, t), \qquad \Gamma = C, C\gamma_5, C\gamma_\mu, C\gamma_\mu\gamma_5$$

$$W(\mathbf{R}) \equiv \lim_{t\to\infty} W(\mathbf{R}, t).$$

今回は scalar diquark の S-wave scattering states に注目するので wave function は A_1^+-wave function に project する

POTENTIALの導出②

- **Schroedinger-type equation**

$$\left(\frac{\mathbf{p}^2}{2\mu} + V(\mathbf{R}) - E\right)W(\mathbf{R}) = 0.$$

RESULTS①

- **Mass**

TABLE I. All the hadronic masses are listed. The masses at $\kappa = 0.1150$ and 0.1250 are obtained without high-energy gluons. (See Sec. V B.) Δm represents the scalar-axialvector-diquark mass splitting.

κ	Scalar	Axialvector	Pseudoscalar	Vector	Δm
0.1350	1.044(2)	1.056(2)	1.285(2)	1.286(3)	0.012(2)
0.1400	0.836(2)	0.855(2)	1.102(2)	1.102(4)	0.019(2)
0.1450	0.618(2)	0.651(2)	0.919(4)	0.918(5)	0.033(2)
0.1500	0.377(3)	0.447(2)	0.757 (7)	0.728(4)	0.070(3)
0.1150	1.020(2)	1.026(2)	1.397(9)	1.352(8)	0.006(2)
0.1250	0.494(2)	0.504(1)	1.053(25)	0.889(19)	0.010(2)

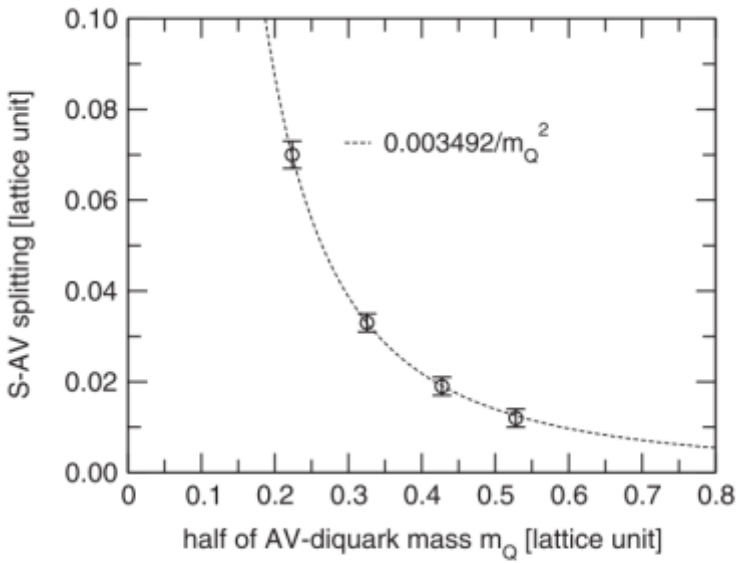

FIG. 1. Scalar-axialvector mass splitting is plotted as a function of axialvector-diquark mass. The dotted line is a fit function Cm_Q^{-2}.

$$\Delta m = Cm_Q^{-2}$$

$$\Delta m = m_{AV} - m_S \quad m_Q = \frac{1}{2} m_{AV}$$

Color-magnetic interaction

RESULTS②

- **Wave function (i, j, k, l) = (1, 2, 1, 2) , (1, 2, 3, 4) (same mass)**

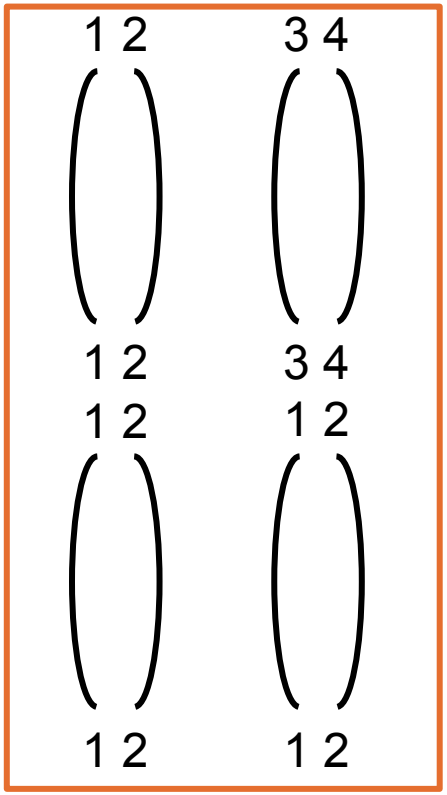

direct diagram

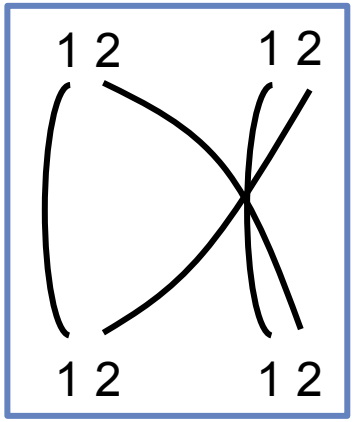

quark-exchange diagram

RESULTS③

- **Wave function:** t≥25

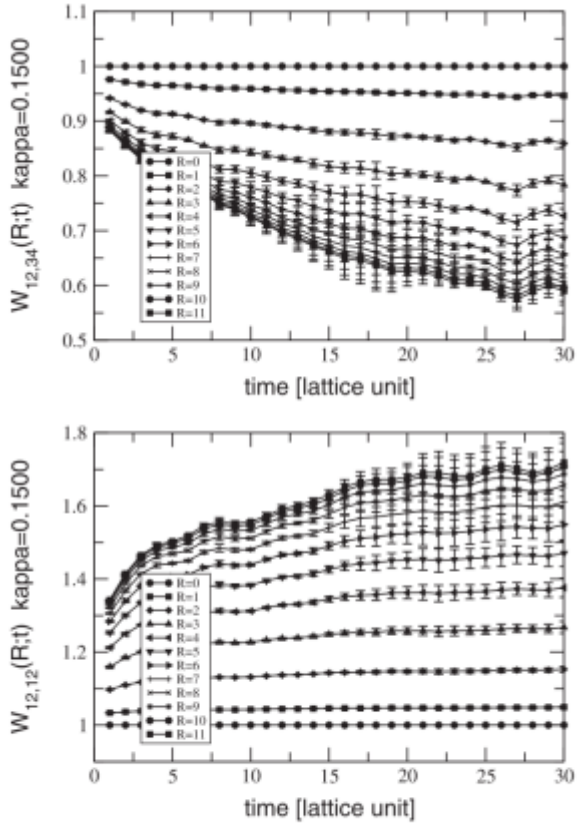

FIG. 2. The wavefunctions $W(R, t)$ at $\kappa = 0.1500$ are plotted as a function of a source-sink separation t.

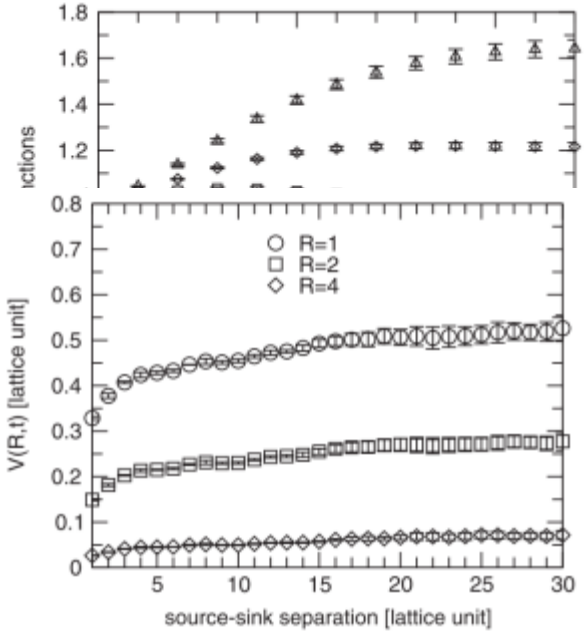

FIG. 3. The potentials $V(R, t)$ at $\kappa = 0.1500$ and $R = 1, 2, 4$ are plotted as a function of a source-sink separation t.

RESULTS④

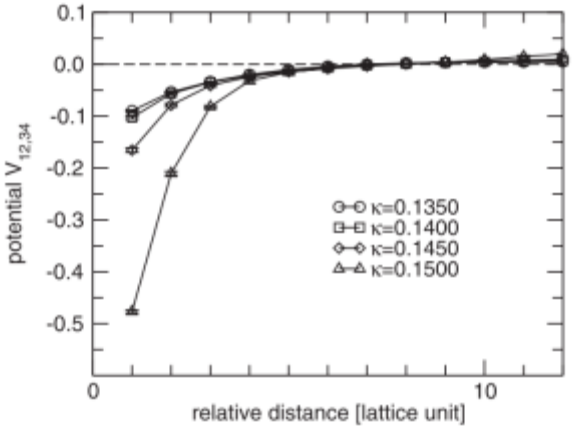

FIG. 5. Potentials $V_{12,34}(R)$ computed with the flavor combination, $(i, j, k, l) = (1, 2, 3, 4)$, are plotted as functions of relative distance R.

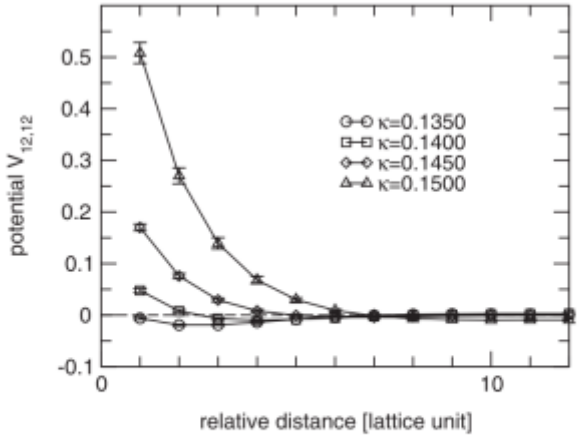

FIG. 6. Potentials $V_{12,12}(R)$ computed with the flavor combination, $(i, j, k, l) = (1, 2, 1, 2)$, are plotted as functions of relative distance R.

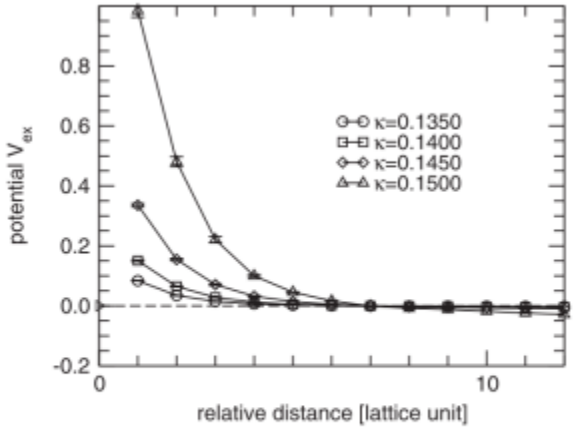

FIG. 7. Quark-exchange parts of potentials, which are defined as $V_{ex}(R) \equiv V_{12,12}(R) - V_{12,34}(R)$, are plotted as functions of relative distance R.

$$V_{ex}(R, m_q) = V_{12,12}(R, m_q) - V_{12,34}(R, m_q)$$

quark-exchange part が
replusive の orign ?

RESULTS⑤

- Potential を以下の関数で fitting

$$F_1(x) \equiv A \frac{\exp(-(\frac{x}{B})^2)}{\sqrt{\frac{x}{B}}}$$

$$F_2(x) \equiv A \frac{\exp(-(\frac{x}{B})^2)}{\frac{x}{B}}$$

$$F_3(x) \equiv A \exp\left(-\frac{x}{B}\right)$$

$$F_4(x) \equiv A \frac{\exp(-\frac{x}{B})}{\sqrt{\frac{x}{B}}}$$

$$F_5(x) \equiv A \frac{\exp(-\frac{x}{B})}{\frac{x}{B}}$$

TABLE II. The best-fit parameters for $V_{ex}(R, m_q)$, $V_{dir}(R, m_q)$, and $V_{att}^D(R, m_q)$. $A(F_i)$ and $B(F_i)$ denote the strength and the range estimated with the function F_i.

V_{dir}	0.1350	0.1400	0.1450	0.1500
$\chi^2/N_{df}(F_1)$	1.462	1.719	12.24	3.163
$\chi^2/N_{df}(F_2)$	54.50	6.970	0.381	9.037
$\chi^2/N_{df}(F_3)$	8.938	1.094	3.516	2.206
$\chi^2/N_{df}(F_4)$	33.78	3.725	0.094	11.33
$\chi^2/N_{df}(F_5)$	85.32	15.00	3.818	30.43
$A(F_1)$	0.046(001)	0.050(002)	0.081(009)	0.345(007)
$A(F_2)$	0.015(004)	0.017(003)	0.032(001)	0.144(010)
$A(F_3)$	0.154(010)	0.171(006)	0.294(019)	1.134(024)
$A(F_4)$	0.073(013)	0.083(008)	0.162(002)	0.655(050)
$A(F_5)$	0.011(008)	0.015(007)	0.046(007)	0.206(052)
$B(F_1)$	4.24(006)	4.33(011)	3.87(024)	2.58(005)
$B(F_2)$	7.06(150)	6.77(076)	5.36(010)	3.61(020)
$B(F_3)$	1.93(008)	1.91(005)	1.62(007)	1.16(002)
$B(F_4)$	3.27(041)	3.11(021)	2.42(002)	1.72(011)
$B(F_5)$	10.3(060)	8.12(277)	4.63(050)	3.20(058)
V_{ex}	0.1350	0.1400	0.1450	0.1500
$\chi^2/N_{df}(F_1)$	3.869	5.317	6.064	7.543
$\chi^2/N_{df}(F_2)$	0.546	1.144	3.713	4.562
$\chi^2/N_{df}(F_3)$	0.095	0.481	0.737	2.202
$\chi^2/N_{df}(F_4)$	1.871	4.896	8.627	13.19
$\chi^2/N_{df}(F_5)$	8.460	16.28	27.94	33.92
$A(F_1)$	0.060(003)	0.099(006)	0.209(012)	0.565(036)
$A(F_2)$	0.025(001)	0.046(002)	0.094(006)	0.277(016)
$A(F_3)$	0.201(002)	0.354(008)	0.744(017)	2.188(085)
$A(F_4)$	0.119(007)	0.223(020)	0.453(046)	1.424(163)
$A(F_5)$	0.040(010)	0.089(023)	0.168(050)	0.606(152)
$B(F_1)$	2.58(010)	2.78(010)	2.99(010)	3.25(007)
$B(F_2)$	3.58(008)	3.63(009)	3.95(015)	3.97(009)
$B(F_3)$	1.14(001)	1.17(002)	1.27(002)	1.29(002)
$B(F_4)$	1.67(008)	1.64(009)	1.80(012)	1.72(008)
$B(F_5)$	2.98(048)	2.61(041)	2.98(055)	2.60(030)
V_{att}^D	0.1350	0.1400	0.1450	0.1500
$\chi^2/N_{df}(F_3)$	N/A	N/A	1.338	0.246
$A(F_3)$	N/A	N/A	0.186(024)	1.041(046)
$B(F_3)$	N/A	N/A	1.05(009)	1.01(004)

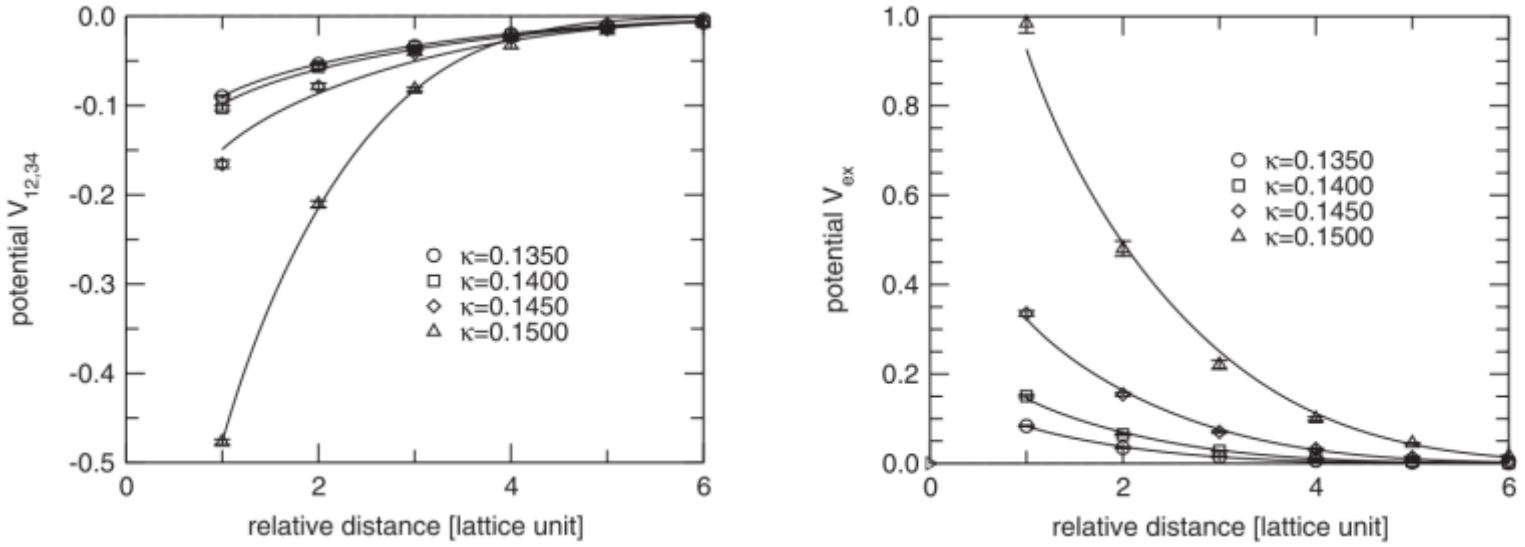

FIG. 8. *Upper*: Attractive parts of potentials, $V_{\rm dir}(R, m_q) = V_{12,34}(R, m_q)$, together with the best-fit curves $F_3(R)$ are plotted as functions of relative distance R. *Lower*: Quark-exchange parts of potentials, $V_{\rm ex}(R, m_q) = V_{12,12}(R, m_q) - V_{12,34}(R, m_q)$, together with the best-fit curves are plotted as functions of relative distance R.

RESULTS⑥

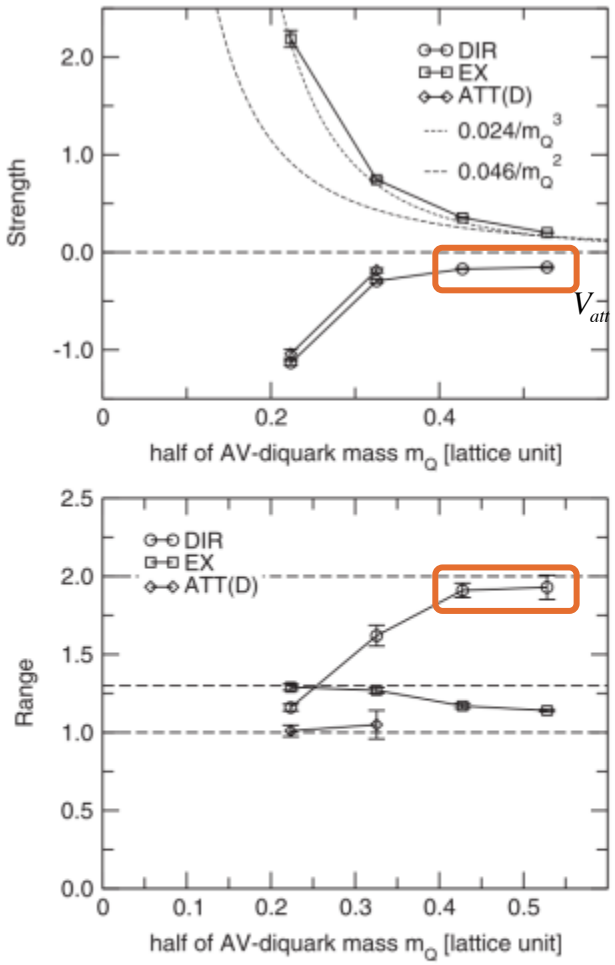

FIG. 9. *Upper*: The fitted strengths, $A_{\rm dir}$, $A_{\rm ex}$, and $A^D_{\rm att}$, of the potentials, $V_{\rm dir}(R, m_q)$, $V_{\rm ex}(R, m_q)$, and $V^D_{\rm att}(R, m_q)$, are plotted as functions of half of axialvector-diquark mass. *Lower*: The fitted interaction ranges, $B_{\rm dir}$, $B_{\rm ex}$, and $B^D_{\rm att}$, of the potentials, $V_{\rm dir}(R, m_q)$, $V_{\rm ex}(R, m_q)$, and $V^D_{\rm att}(R, m_q)$. The parameters for $V_{\rm dir}(R, m_q)$, $V_{\rm ex}(R, m_q)$, and $V^D_{\rm att}(R, m_q)$ are, respectively, shown as DIR, EX, and "ATT(D)".

heavy-quark-mass region で flat になっている

V_{dir} には "universal" な attractive potential V^U_{att} が含まれるのでは？

"universal" = strength も range も mass に依らず、あらゆる flavor channel で現れる

$$V^U_{att}(R, m_q) = V_{dir}(R, \kappa = 0.1350)$$

$$V^D_{att}(R, m_q) = V_{dir}(R, m_q) - V^U_{att}(R)$$

$$V_{\rm dir}(R, m_q) \sim V^U_{\rm att}(R) + V^D_{\rm att}(R, m_q)$$

$$= A^U_{\rm att} f^U_{\rm att}(R) + A^D_{\rm att}(m_q) f^D_{\rm att}(R).$$

$$V_{\rm ex}(R, m_q) \sim A_{\rm ex}(m_q) f_{\rm ex}(R).$$

REMOVAL OF HIGH-MOMENTUM GLUONS①

- **Fourier transform を用いた link variable の high-momentum cut**

A. Yamamoto and H. Suganuma, Phys. Rev. Lett. 101, 241601(2008)
A. Yamamoto and H. Suganuma, Phys. Rev. D 79, 054504(2009)
A. Yamamoto, Phys. Lett. B 688, 345(2010)

$$U_\mu(\mathbf{p}, t) = \sum_{\mathbf{x}} U_\mu(\mathbf{x}, t) e^{i\mathbf{p}\cdot\mathbf{x}}.$$

$$\tilde{U}_\mu^{\text{low}}(\mathbf{p}, t) = \begin{cases} U_\mu(\mathbf{p}, t) & (|\mathbf{p}| \le \Lambda) \\ 0 & \text{otherwise} \end{cases}$$

$$\tilde{U}_\mu^{\text{low}}(\mathbf{x}, t) \equiv \frac{1}{V} \sum_{\mathbf{p}} \tilde{U}_\mu^{\text{low}}(\mathbf{p}, t) e^{-i\mathbf{p}\cdot\mathbf{x}}$$

$$\text{Tr}\,(U_\mu^{\text{low}}(\mathbf{x}, t) - \tilde{U}_\mu^{\text{low}}(\mathbf{x}, t))(U_\mu^{\text{low}}(\mathbf{x}, t) - \tilde{U}_\mu^{\text{low}}(\mathbf{x}, t))^\dagger,$$

これを最小化するU^{low}_μを新しい link variableとして採用

今回は Λ=5 とした

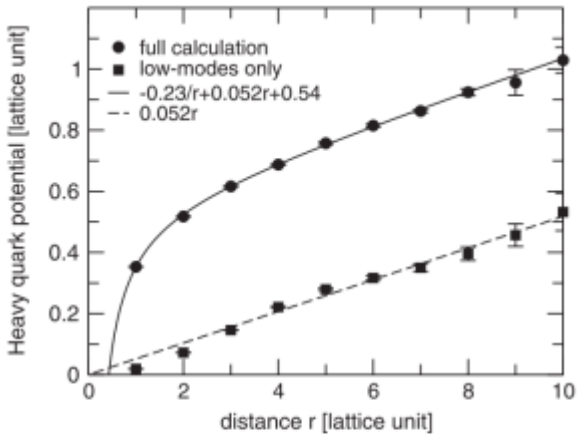

FIG. 11. Heavy-quark-antiquark potential as a function of a separation r. The upper data shown as circles denote the lattice QCD data obtained in full SU(2) calculation, and the lower data shown as squares denote those obtained without high-momentum gluons. The infrared cut Λ is set to $\Lambda = 5$ in lattice unit. The original $Q\bar{Q}$ potential is fitted as $V_{Q\bar{Q}}(r) = -0.2397(53)\frac{1}{r} + 0.0518(10)r + 0.5405(50)$.

REMOVAL OF HIGH-MOMENTUM GLUONS②

TABLE I. All the hadronic masses are listed. The masses at $\kappa = 0.1150$ and 0.1250 are obtained without high-energy gluons. (See Sec. V B.) Δm represents the scalar-axialvector-diquark mass splitting.

κ	Scalar	Axialvector	Pseudoscalar	Vector	Δm
0.1350	1.044(2)	1.056(2)	1.285(2)	1.286(3)	0.012(2)
0.1400	0.836(2)	0.855(2)	1.102(2)	1.102(4)	0.019(2)
0.1450	0.618(2)	0.651(2)	0.919(4)	0.918(5)	0.033(2)
0.1500	0.377(3)	0.447(2)	0.757 (7)	0.728(4)	0.070(3)
0.1150	1.020(2)	1.026(2)	1.397(9)	1.352(8)	0.006(2)
0.1250	0.494(2)	0.504(1)	1.053(25)	0.889(19)	0.010(2)

high-momentum-gluon cut 後のΔmがかなり小さくなるκを用意

Color magnetic interaction が抑制されている状況

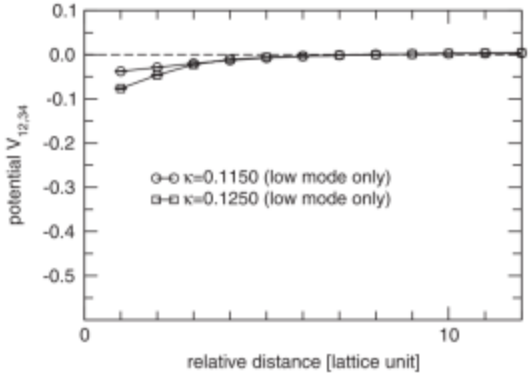

FIG. 12. Potentials $V_{12,34}(R)$ for the flavor combination $(i, j, k, l) = (1, 2, 3, 4)$ computed without high-momentum gluons are plotted as functions of relative distance R. The infrared cut Λ is set to $\Lambda = 5$ in lattice unit.

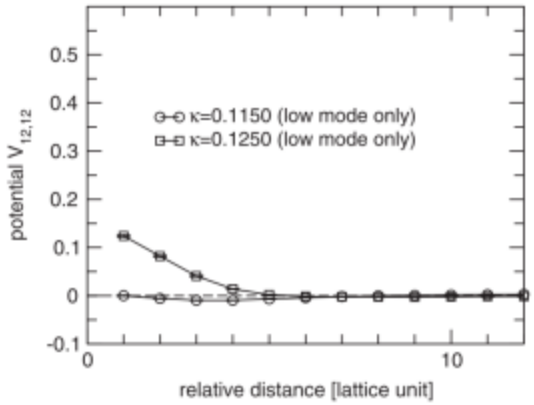

FIG. 13. Potentials $V_{12,12}(R)$ for the flavor combination $(i, j, k, l) = (1, 2, 1, 2)$ computed without high-momentum gluons are plotted as functions of relative distance R. The infrared cut Λ is set to $\Lambda = 5$ in lattice unit.

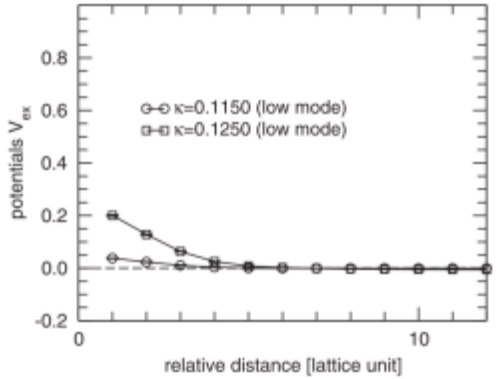

FIG. 14. Quark-exchange parts of potentials, which are defined as $V_{ex}(R) \equiv V_{12,12}(R) - V_{12,34}(R)$, computed without high-momentum gluons are plotted as functions of relative distance R. The infrared cut Λ is set to $\Lambda = 5$ in lattice unit.

REMOVAL OF HIGH-MOMENTUM GLUONS③

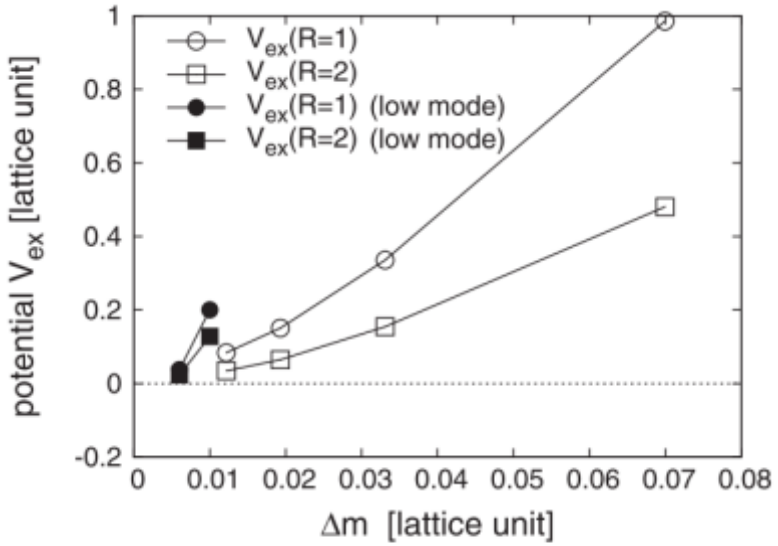

FIG. 15. The values of V_{ex} at $R = 1$ and 2 are plotted as functions of S-AV mass splitting Δm.

Cut によって CM interaction が抑制されたが、repulsive force は必ずしも減少するわけではない

OPERATOR DEPENDENCE OF THE POTENTIAL①

- **BS amplitude の sink 側の operator を smearing**

$$q_b(\mathbf{x};\mathbf{r}) \equiv \prod^{N}\left(1+\alpha\sum_{i=1}^{3}K_i(U)_{\mathbf{xy}}\right)\delta_{\mathbf{y},\mathbf{r}}. \qquad K_\mu(U)_{xy} \equiv U_\mu^\dagger(x)\delta_{x+\hat{\mu},y} + U_\mu(x-\hat{\mu})\delta_{x-\hat{\mu},y}$$

α,Nは分布の半径がbになるように選ぶ

$$H_b(\mathbf{x_1},\mathbf{x_2};\mathbf{x}) = q_{1,b}(\mathbf{x_1};\mathbf{x})q_{2,b}(\mathbf{x_2};\mathbf{x}).$$

⇒ $(x_1+x_2)/2=x$ 以外の寄与をなくしたい

$$U_\mu^{\theta_\mu} \equiv \exp(i\theta_\mu)U_\mu \qquad 0 \le \theta_\mu < 2\pi$$

$$K_\mu^{\theta_\mu}(U)_{xy} \equiv U_\mu^{\theta_\mu\dagger}(x)\delta_{x+\hat{\mu},y} + U_\mu^{\theta_\mu}(x-\hat{\mu})\delta_{x-\hat{\mu},y} = \exp(-i\theta_\mu)U_\mu^\dagger(x)\delta_{x+\hat{\mu},y} + \exp(i\theta_\mu)U_\mu(x-\hat{\mu})\delta_{x-\hat{\mu},y}.$$

$$q_b^{\vec{\theta}}(\mathbf{x};\mathbf{r}) \equiv \prod^{N}\left(1+\alpha\sum_{i=1}^{3}K_i^{\theta_i}(U)_{\mathbf{xy}}\right)\delta_{\mathbf{y},\mathbf{r}} = \exp(i\vec{\theta}\cdot(\mathbf{x}-\mathbf{r}))q_b(\mathbf{x};\mathbf{r}).$$

簡単のため $\mathbf{x}=\mathbf{0}$ とする

$$H_b^{\vec{\theta}}(\mathbf{x_1},\mathbf{x_2};\mathbf{0}) = \exp(i\vec{\theta}\cdot(\mathbf{x_1}+\mathbf{x_2}))q_{1,b}(\mathbf{x_1};\mathbf{0})q_{2,b}(\mathbf{x_2};\mathbf{0}).$$

⇒ で和を取れば $(x_1+x_2)/2=0$ にできる

OPERATOR DEPENDENCE OF THE POTENTIAL②

- **The root-mean-square radius b の決定**

$$c_i \equiv \langle \mathrm{vac} | D_{ij,\Gamma} | i\text{th state} \rangle.$$

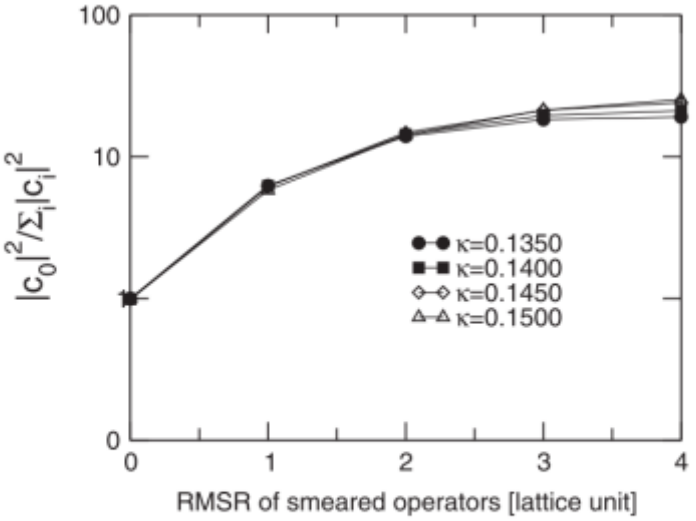

FIG. 16. $|c_0|^2/\sum_i |c_i|^2$ are plotted as a function of the RMSR of a smeared operator b_{smr}. Here, c_i denotes the overlap of a diquark operator and i-th state; $c_i \equiv \langle \mathrm{vac} | D_{ij,\Gamma} | i\text{th state} \rangle$.

b_{smr}=3とした

OPERATOR DEPENDENCE OF THE POTENTIAL③

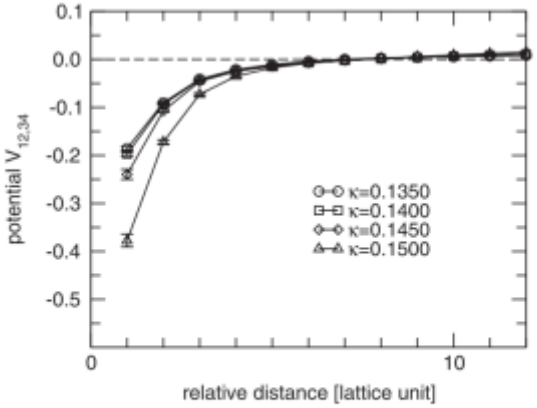

FIG. 17. Potentials $V_{12,34}(R)$ computed with projected smeared diquark operators $\sum_{\vec{\theta}} H_b^{\vec{\theta}}$, with the flavor combination, $(i, j, k, l) = (1, 2, 3, 4)$, are plotted as functions of relative distance R.

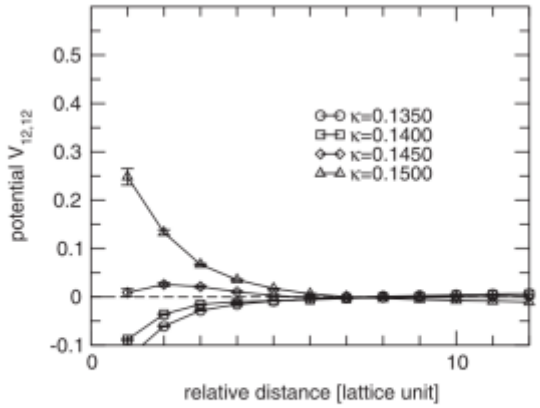

FIG. 18. Potentials $V_{12,12}(R)$ computed with projected smeared diquark operators $\sum_{\vec{\theta}} H_b^{\vec{\theta}}$, with the flavor combination, $(i, j, k, l) = (1, 2, 1, 2)$, are plotted as functions of relative distance R.

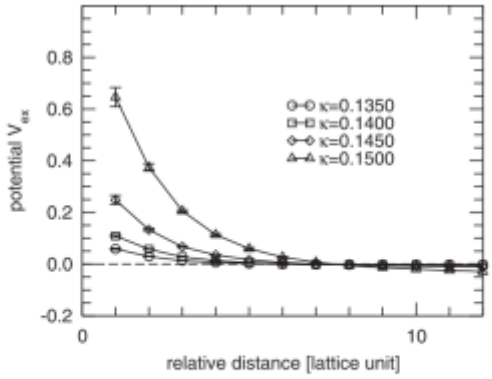

FIG. 19. Quark-exchange parts of potentials, which are defined as $V_{ex}(R) \equiv V_{12,12}(R) - V_{12,34}(R)$, are plotted as functions of relative distance R. In this case, $V_{12,12}(R)$ and $V_{12,34}(R)$ are those measured with projected smeared diquark operators $\sum_{\vec{\theta}} H_b^{\vec{\theta}}$.

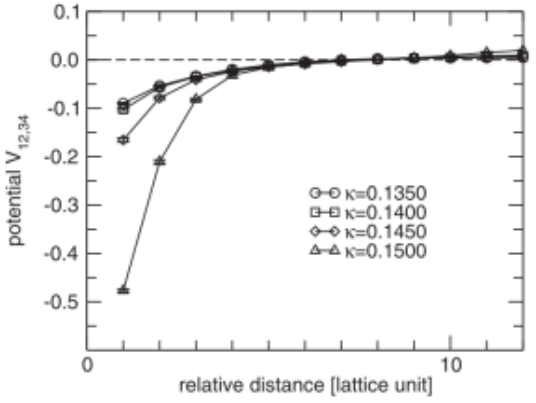

FIG. 5. Potentials $V_{12,34}(R)$ computed with the flavor combination, $(i, j, k, l) = (1, 2, 3, 4)$, are plotted as functions of relative distance R.

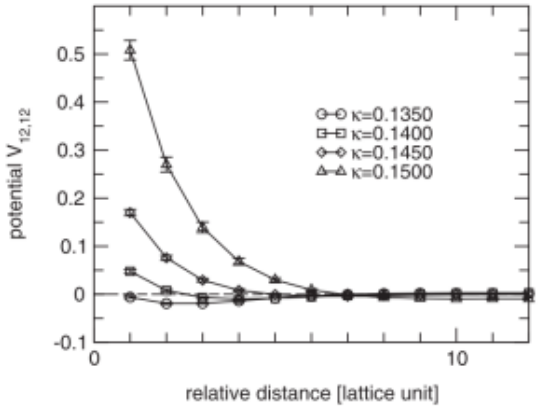

FIG. 6. Potentials $V_{12,12}(R)$ computed with the flavor combination, $(i, j, k, l) = (1, 2, 1, 2)$, are plotted as functions of relative distance R.

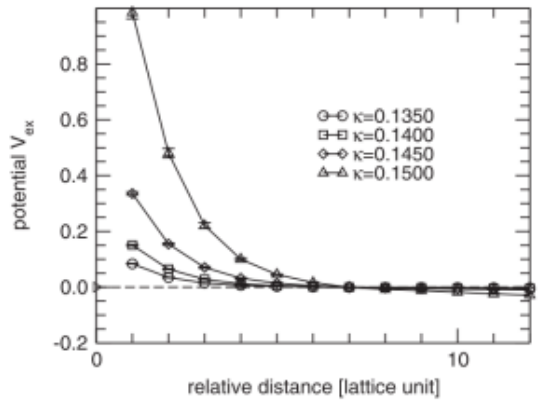

FIG. 7. Quark-exchange parts of potentials, which are defined as $V_{ex}(R) \equiv V_{12,12}(R) - V_{12,34}(R)$, are plotted as functions of relative distance R.

OPERATOR DEPENDENCE OF THE POTENTIAL④

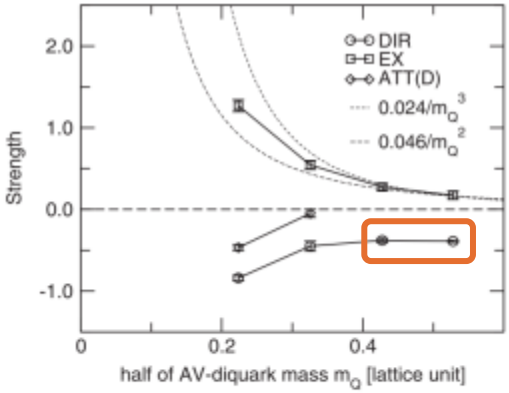

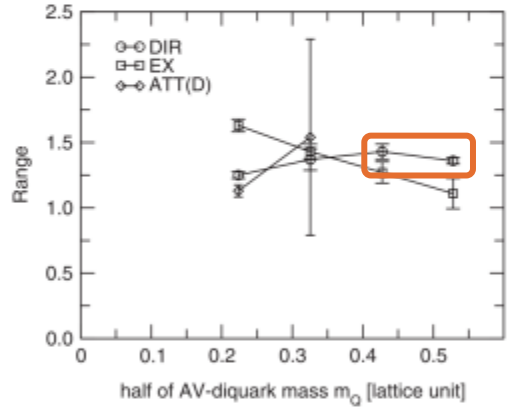

FIG. 20. *Upper*: The fitted strengths, $A_{\rm dir}$, $A_{\rm ex}$, and $A^D_{\rm att}$, of the potentials, $V_{\rm dir}(R, m_q)$, $V_{\rm ex}(R, m_q)$, and $V^D_{\rm att}(R, m_q)$, are plotted as functions of half of axialvector-diquark mass. *Lower*: The fitted interaction ranges, $B_{\rm dir}$, $B_{\rm ex}$, and $B^D_{\rm att}$, of the potentials, $V_{\rm dir}(R, m_q)$, $V_{\rm ex}(R, m_q)$, and $V^D_{\rm att}(R, m_q)$. The parameters for $V_{\rm dir}(R, m_q)$, $V_{\rm ex}(R, m_q)$, and $V^D_{\rm att}(R, m_q)$ are, respectively, shown as DIR, EX, and "ATT(D)". All the parameters are obtained by fitting potentials measured with projected smeared diquark operators $\sum_{\vec{a}} H^{\vec{a}}_b$.

Universal attraction が存在している

SUMMARY

- quenced two-color lattice QCD で potential V(R) を計算
- Four flavor(same mass), various quark mass で repulsive force の起源を探った

$$V_{ex}(R, m_q) = V_{12,12}(R, m_q) - V_{12,34}(R, m_q)$$

- Potential の operator dependence を見た
- Operator independent なものも見えた

1. Universal attraction が存在
2. いずれの でも V_{ex}は repulsive